Sodium hypochlorite sensing by different size of optical micro-bottle resonators

MD ASHADI MD JOHARI[a,*], MOHD HAFIZ BIN JALI[b], HAZIEZOL HELMI BIN MOHD YUSOF[c], HAZLI RAFIS BIN ABDUL RAHIM[c], AMINAH BINTI AHMAD[a], MUHAMMAD IMRAN MUSTAFA ABDUL KHUDUS[d], SULAIMAN WADI HARUN[e]

[a]*Faculty of Electrical and Electronic Engineering Technology, Universiti Teknikal Malaysia Melaka, 76100 Melaka, Malaysia*

[b]*Faculty of Electrical Engineering, Universiti Teknikal Malaysia Melaka, 76100 Melaka, Malaysia*

[c]*Faculty of Electronic and Computer Engineering, Universiti Teknikal Malaysia Melaka, 76100 Melaka, Malaysia*

[d]*Department of Physics, Faculty of Science, University of Malaya, 50603 Kuala Lumpur, Malaysia*

[e]*Department of Electrical Engineering, Faculty of Engineering, University of Malaya, 50603 Kuala Lumpur, Malaysia*

This paper studied whispering gallery modes on the micro bottle resonator (MBR) as sodium hypochlorite sensor. The MBR designed by method "soften-and-compress" in three different bottle diameters. The parameters named as bottle diameter D_b, stem diameter of D_s and bottle length of L_b. The Q-factor defined by coupled with tapered microfiber with $2\mu m$ diameter and succeeded to have $> 10^5$. The range of sodium hypochlorite concentrations from 1% pmm to 6% pmm was then used for analysis purpose. The performance of the MBRs undeniably excellent with sensitivity linearity and repeatability analysed from wavelength shift and transmitted power.

(Received March 3, 2021; accepted October 7, 2021)

Keywords: Optical Microresonator, Microbottle Resonator, Sodium Hypochlorite

1. Introduction

Optical microresonator (OMRs) with whispering gallery modes (WGMs) captured interest recently due to wide applications in laser, sensor or related plasmonic devices, which captured interest recently [1-7]. OMRs narrow modes in spatially and temporally, enabling high optical intensities, a broad quality factor and extending photon lifetimes in the resonator structure to be generated and realised in several different forms, suc h as micropillars microdisks, microrings and photonic-crystal cavities [8-11]. WGMs OMRs intensively researched, various advantages such as high qu ality factor, low intrinsic loss and easy manufacturing tech niques have also been seen [12]. One of OMR substructure is the microbottle resonator (MBR), formed by the silica fiber by increasing the midriff area's size until forming a bump structure, which similar to bottle structure. The MBR was operating when the WGMs ware was continually circulating across the MBR surface perpendicular to the bottle axis. The electromagnetic field was established around the MBR surface, useful for sensing the application [13-17]. This explanation is similar to the surface plasmon-polaritons (SPPs) electromagnetic field [18, 19]. However, the MBR was suggested to be suitable for OMR sensors based on silica because they have a very high quality factor and a free spectral range (FSR) [20, 21]. We advocated using the MBR with different size as sodium hypochlorite sensing. Previously, the MBR with different numbers and sizes was used for humidity, temperature, and formaldehyde sensing by observing sensor sensitivity [13, 22, 23]. Hance, non-other previous studies on the performance of the MBR with different size for sodium hypochlorite sensing. The MBR may be fabricated by two technique such as “soften-and-compress” and “heat-and-pull” [24, 25]. Due to the handling procedure and the size of resonator need by the experiment, the MBR structured using the "soften-and-compress" technique from SMF-28 silica fibre, which combined with the 2 μm wrist diameter taper microfiber to perform sensing [26]. Hence, the MBR diameter changes were influenced by a different shifting of wavelength, which led to the MBR absorption capability of sodium hypochlorite particle. By theoretical study, introducing a larger MBR size will increase the quality factor and lead to high sensitivity while performing liquid sensing. The experiment is conducted in a sealed chamber with sodium hypochlorite concentrations ranging from 1% to 6% ppm. The MBR purposed showed a high sensitivity, consistency repeatability and stable performance test were founded during the experiment.

2. Characterisation of MBR

The MBR is created from a standard silica fiber SMF-28 using a stable technique called "soften-and-compress", were potentially used by whispering gallery modes to

modifying spectral characterisation [26]. The SMF-28 fiber was held and compress inward direction on both sides using the splicing machine (Furukawa Electric Fitel S178A) after being heated with an electrical arc. The bottle's size is determined by the number of arcs applied during the process to the centre of heated fiber [20]. Fig. 1 shows the structure of the MBR, which characterised by three parameters known as the neck-to-neck length L_b, the bottle diameter D_b and the stem diameter D_s which is slightly same with other previous works [20]. The microfiber with a waist diameter of 2 μm is fabricated flame brushing technique were used to be employ with the MBR [27]. Table 1 showed three different size of MBR used as sodium hypochlorite concentrations sensor. When the bottle size D_s increasing, the stem diameter D_s remained the same while neck-to-neck L_b decrease in small numbers.

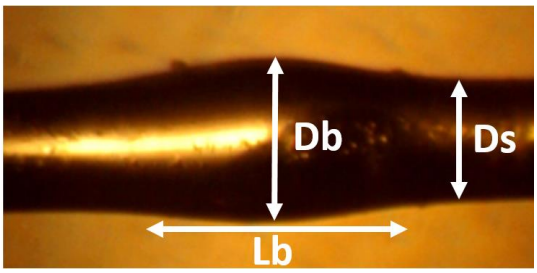

Fig. 1. Sample fabricated MBR of L_b = 197 μm, D_b = 180 μm and D_s = 125 μm (color online)

Table 1. The MBR in three different sizes

Micro-bottle Resonator	Neck-To-Neck Length L_b	Bottle Diameter D_b	Stem Diameter D_s
A	**200μm**	170μm	125μm
B	**197μm**	180μm	125μm
C	**194μm**	190μm	125μm

The MBR with three sizes is employed toward tapered microfiber with 2μm tapering size for characterisation procedure using a wavelength range from 1552.0 nm to 1552.3 nm, supplied from a tunable laser source (TLS) (ANDO AQ4321D). The capability of a tunable laser source to produce wavelength between 1520 nm until 1620 nm with a 0.001 nm interval was perfectly matched with this experiment's need. The transmitted power wavelength from the tunable laser source will finally be collected by an optical power meter (OPM) (THORLABS S145C) as output data. The transmission spectral of the various MBR sizes shown in Fig. 2 was used to define the quality factor [28]. The MBRs have different insertion loss values: -7 dBm for A size, -13 dBm for B size and -22 dBm for C size. This value may control by controlling the coupling distance between MBR and tapered microfiber [29]. Insertion loss occurred due to free-space radiation modes, larger numbers of partially overlapping and over-couple of WGMs where direct contact of the MBR with tapered microfiber [28]. The different size of the MBR lead to have different transmitted spectral with numbers of resonance depth.

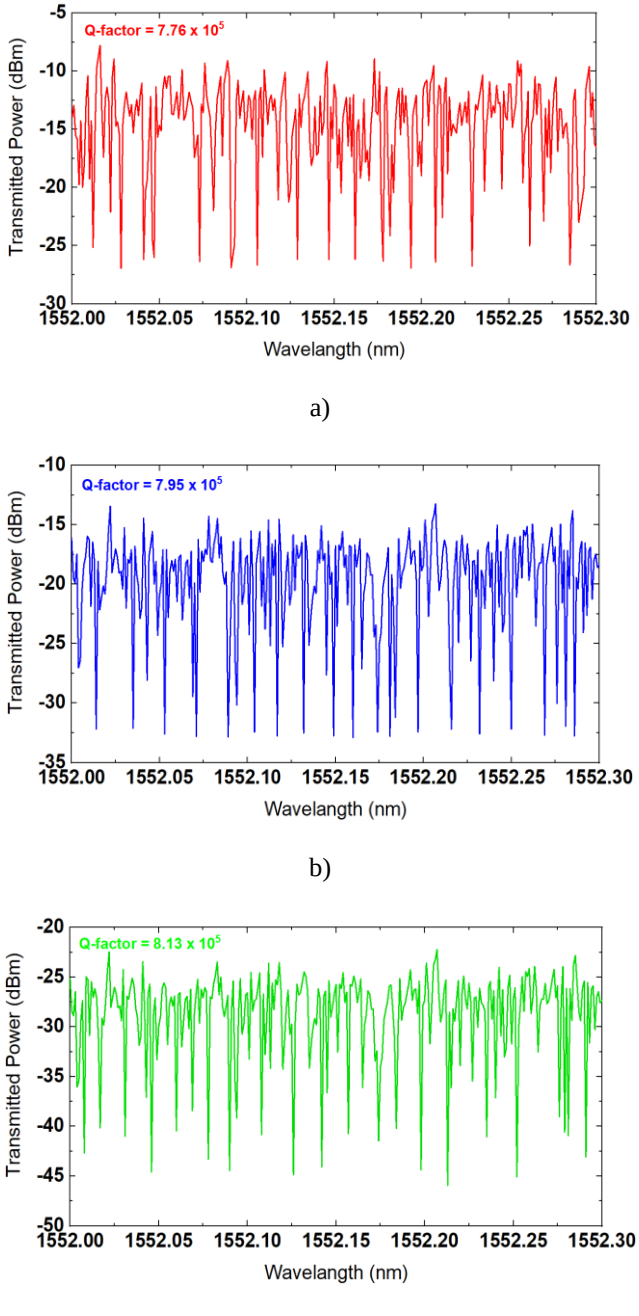

Fig. 2. The transmitting spectral of the different size MBR and the 2μm tapered microfiber with numbers of WGM resonating (color online)

The Q-factor was defined for all MBR size by calculation and Lorentzian fitting, where all are found to have $> 10^5$ which is similar to previous research [13, 20]. By calculation, Q-factor is defined from $\lambda/\Delta\lambda$ where λ define as resonant wavelength. The Lorentzian fitting is define from Origin software used. As Fig. 4, size A of MBR manage to have 7.76×10^5 which is smallest than size B of MBR and size C of MBR were able to have 7.95×10^5 and 8.13×10^5 respectively. The Q-factor may increase when the biggest size of the MBR is used [28]. The insertion loss changed due to the coupling gap with the microfiber, free-radian modes and numbers of partial overlapping [30, 31]. The free spectral range (FSR) defined as slightly different for each MBRs with size A is 0.015 nm, size B is 0.011 nm, and size C is 0.10 nm. The lowest FSR value by size C showed that this MBR is the best among others.

3. Performance of MBR Sodium Hypochlorite Sensor

Fig. 3 showed the experiment setup used than to examine the performance of MBRs as sodium hypochlorite sensor. The setup is placed in a sealed chamber to ensure the humidity and temperature remain the same. Inside the sealed chamber, the MBR with different size is coupled with tapered microfiber, where one end of microfiber is connected to an optical power meter and tunable laser source to the other end for transmitted power measurement. At first, the wavelength was set to 1552.03 nm, where this was the deepest resonating depth is recorded for size A of MRB. The sodium hypochlorite liquid concentration was then changed from 1% ppm to 6% ppm, and output power is examined for every liquid concentration level. For repeatability investigation of the sodium hypochlorite sensor, the experiment was repeated three times on the same day. The transmission spectral at 6% sodium hypochlorite concentration level was recorded for 120 minutes for the stability test. The experiment was repeated using other MBR, with B and C size, respectively. The input wavelength value used for size B is 1552.16 nm and 1552.22 nm for size C. The different wavelength value was applied for all MBR sizes. Every size managed to have its resonance depth wavelength, which was then used for sodium hypochlorite sensing experiments.

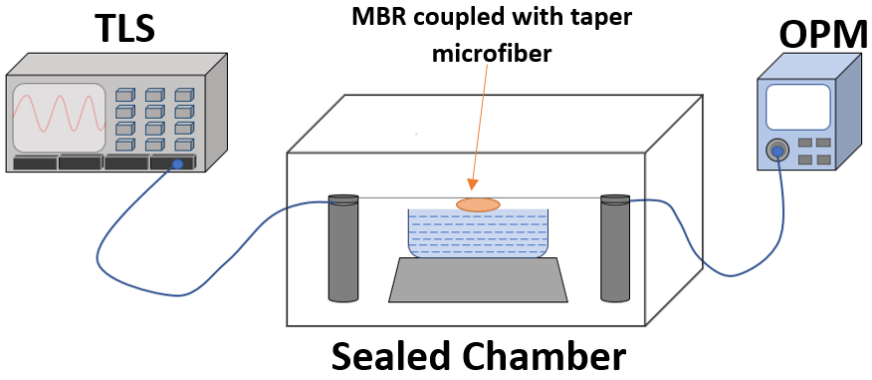

Fig. 3. The MBRs were attached with tapered fiber for sodium hypochlorite sensing (color online)

For analysis on wavelength shift, every size of the MBR, the tuneable laser source transmitted different wavelength range. The range of wavelength previously determined from the Q-factor calculation in Fig. 2. The optical power meter connected to the computer is used to monitors and records spectral wavelength on every concentration level of sodium hypochlorite. For size A, the MBR manage to shift a wavelength from 1552.206 nm to 1552.214 nm, while size B is from 1552.203 nm to 1552.213 nm and size C is from 1552.203 nm to 1552.217 nm, as shown in Fig. 4. The result was obtained because of the adsorption concept where the MBR interaction with sodium hypochlorite liquid particles was changed extremely on every concentration level. It is proved that the MBR practically suitable to decrease the adsorption competency when dealing with sodium hypochlorite liquid sensing.

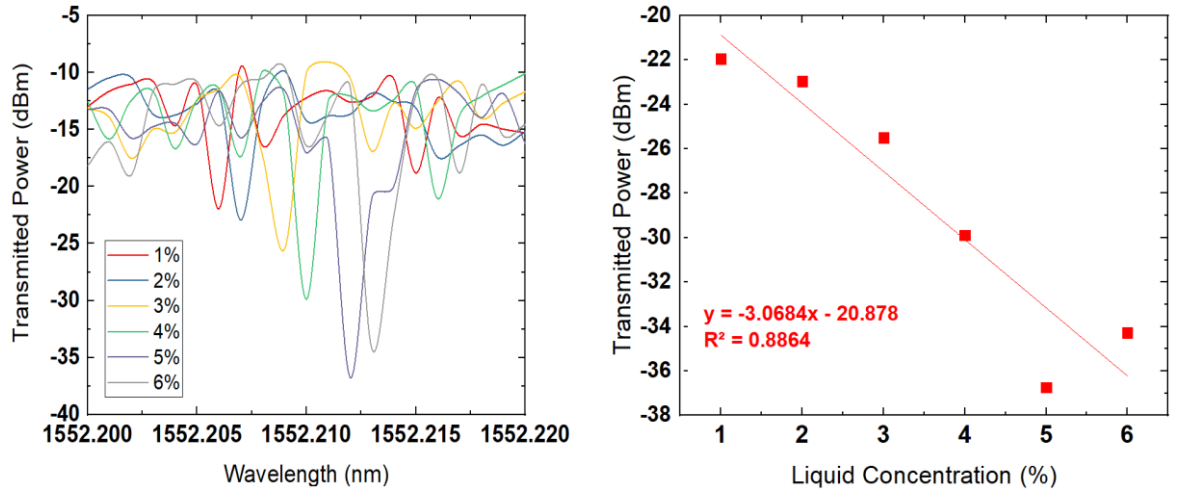

Size A

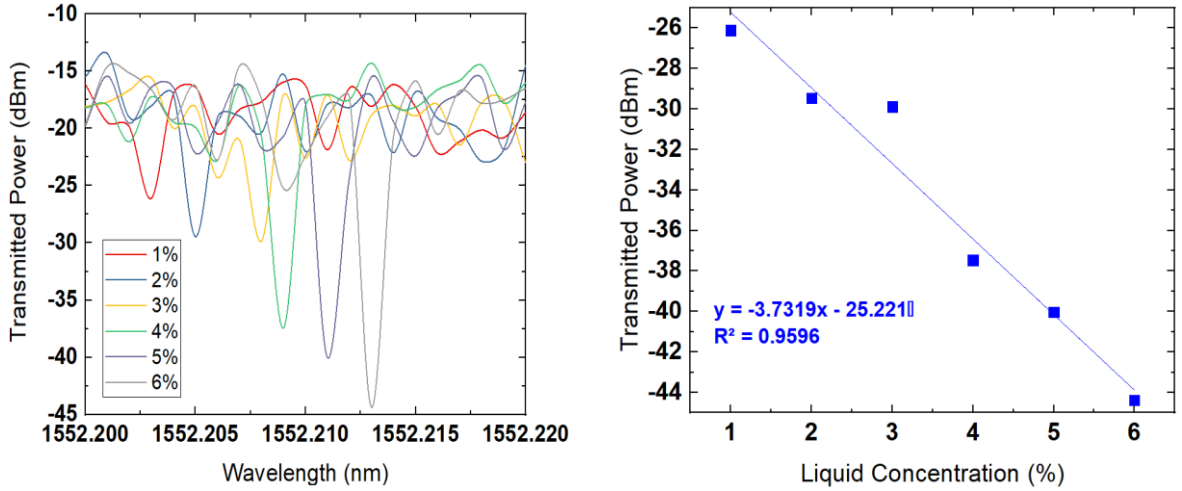

Size B

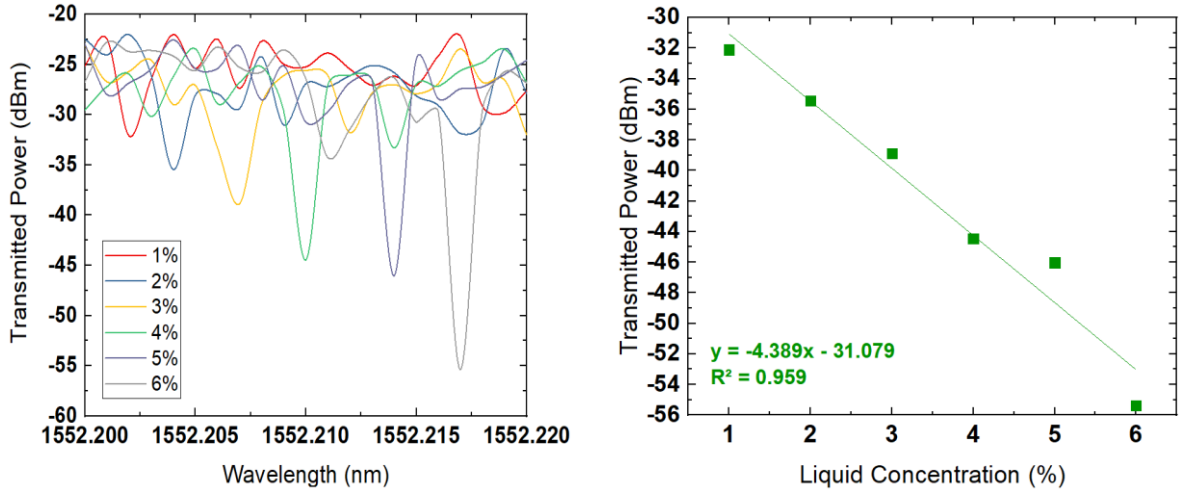

Size C

Fig. 4. The wavelength shifts for three different MBR sizes, leading to defining the sensitivity and linearity results for all conditions (color online)

Fig. 4 showed all the transmitted spectral analysis performance for three different MBR sizes towards different sodium hypochlorite concentration levels recorded. This experiment repeated three times for all sizes of MBR. However, the graph only showed the averaging value of repeatability and placed it together with all other data in the same graph. Based on the graph trend, the transmitted power (dBm) value decreased per unit rise of sodium hypochlorite concentration level. The linear graph slope defined as the sensitivity value of the MBR in different sizes showed that size C to have higher sensitivity 3.684 dB/%ppm than size B 3.7319 dB/%ppm, and size A 4.389 dB/%ppm. The linearity of size A is 94.15%, which lower than size B, 97.96% and size C 97.93%. However, to ensure the size C shows a better performance, the sensitivity and linearity results of all size should be defined by wavelength shift, as shown in Fig. 5**.** The wavelength shifted increased when the sodium hypochlorite concentration level raised. The sensitivity and linearity defined by the slope value of wavelength shifted towards a different sodium hypochlorite concentration level. Size C MBR still became the highest by 3.1 pm/%ppm for sensitivity value and 99.6% for linearity value, which more than size B and size A. Size B manage to have 2.0 pm/%ppm with 99.4% for sensitivity and linearity. In comparison, size C only have 1.5 pm/%ppm with 99.5%.

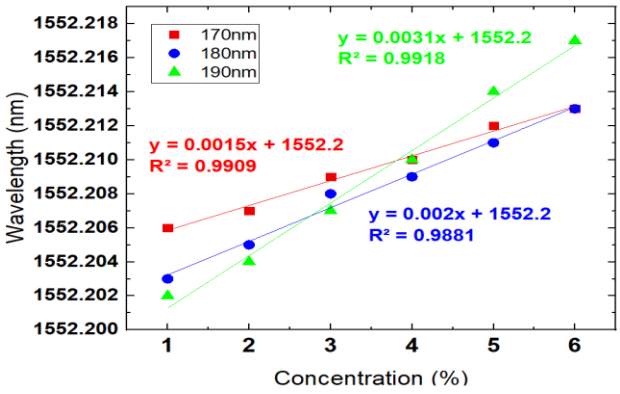

Fig. 5. The wavelength shifts for three different size of MBR (color online)

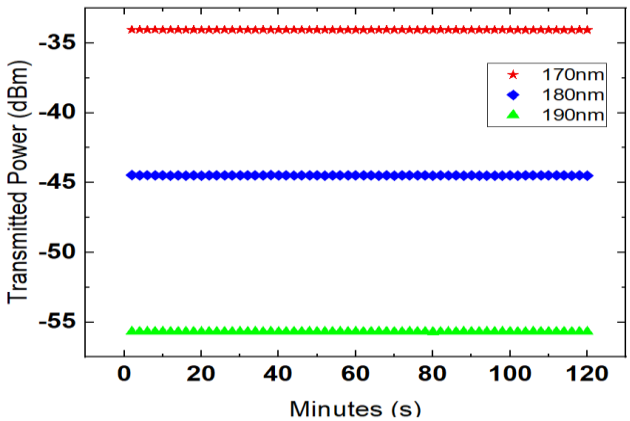

Fig. 6. The stability results of different size of MBR microfiber for sodium hypochlorite sensor (color online)

Fig. 6 record the MBR for three different size stability test results for sodium hypochlorite sensor. The sensing data was taken for 120 minutes at 6% ppm of sodium hypochlorite concentration, where 120 different transmitted power recorded in the time range. Based on the tabulated data shown in Fig. 6, the sodium hypochlorite sensor was performed so stably during the experiment. This ensures the condition of sensor during the experiment remained good, which would be additional information for sensor optimisation. It also assumes that the MBR with three sizes do perform well on data collection.

4. Conclusions

This experimental paper studied the effect of different size MBR microfiber for sodium hypochlorite sensor. The technique established as "soften-and-compress" applied on silica fiber SMF-28 with several arc numbers to form bottle structure with parameters as bottle diameter D_b, stem diameter D_s and bottle length L_b. Three different sizes of MBR are formed. The characterisation of the MBRs defined by using TLS with the wavelength from 1552.00 nm to 1552.30 nm as 0.001 nm interval via 2 μm tapered microfiber. The Q-factor of the MBRs are defined to have $> 10^5$ which was significantly similar to previous works. The performance of the sodium hypochlorite sensor is then compared among between three sizes of the MBRs. Size C was defined to be well performed than size B and size C by sensitivity and linearity analysis. The experiment repeated three-time cycles among three size MBRs to reduce random reading error and stability test for each size to ensure data collection accuracy.

Acknowledgements

The authors would like to acknowledge Fakulti Teknologi Kejuruteraan Elektrik dan Elektronik, Fakulti Kejuruteraan Elektrik, Fakulti Kejuruteraan Elektronik dan Komputer, Universiti Teknikal Malaysia Melaka and Faculty of Engineering, University of Malaya.

References

[1] Korobko, Zolotovskii, Svetukhin, Zhukov, Fomin, Borisova, Fotiadi, Optics Express **28**(4), 4962 (2020).
[2] R. R. Galiev, N. M. Kondratiev, V. E. Lobanov, I. A. Bilenko, Journal of Physics: Conference Series. IOP Publishing **1283**, 012006 (2019).
[3] Tian Xiaoyi, Powell Keith, Li Liwei, Chew Suen Xin, Yi Xiaoke, Nguyen Linh, Minasian Robert A, Journal of Lightwave Technology **38**(19), 5440 (2020).
[4] L. Kelemen, E. Lepera, B. Horváth, P. Ormos, R. Osellame, R. M. Vázquez, Lab on a Chip **19**(11), 1985 (2019).
[5] A. Ahmad, Xiau S. Cheng, Mukul C. Paul, A. Dhar, S. Das, H. Ahmad, S. W. Harun, Microwave and

Optical Technology Letters **61**(1), 173 (2019).
[6] A. Ahmad, Xiau S. Cheng, Mukul C. Paul, A. Dhar, S. Das, H. Ahmad, S. W. Harun, Microwave and Optical Technology Letters **61**(6), 1651 (2019).
[7] A. Ahmad, S. W. Harun, M. C. Paul, M. F. M. Rusdi, S. Das, A. Dhar, K. A. Noordin, Kamarul Ariffin, Microwave and Optical Technology Letters **62**(11), 3634 (2020).
[8] Z. Fang, H. Luo, J. Lin, M. Wang, J. Zhang, R. Wu, J. Zhou, W. Chu, T. Lu, Y. Cheng, Optics Letters **44**(24), 5953 (2019).
[9] S. Anguiano, A. E. Bruchhausen, B. Jusserand, I. Favero, F. R. Lamberti, L. Lanco, L. Sagnes, A. Lemaître, N. D. Lanzillotti-Kimura, P. Senellart, Physical Review Letters **118**(26), 263901 (2017).
[10] M. Zhang, B. Buscaino, C. Wang, A. Shams-Ansari, C. Reimer, R. Zhu, J. M. Kahn, M. Lončar, Nature **568**(7752), 373 (2019).
[11] M. Clementi, K. Debnath, M. Sotto, A. Barone, A. Z. Khokhar, T. D. Bucio, S. Saito, F. Y. Gardes, D. Bajoni, M. Galli, Applied Physics Letters **114**(13), 131103 (2019).
[12] L. Wu, H. Wang, Q. Yang, Q. X. Ji, B. Shen, C. Bao, M. Gao, K. Vahala, Optics Letters **45**(18), 5129 (2020).
[13] M. A. M. Johari, M. I. M. Khudus, M. H. B. Jali, Al Noman, S. W. Harun, Sensors and Actuators A: Physical **284**, 286 (2018).
[14] MAM. Johari, Al Noman, MIMA. Khudus, MH. Jali, HHM Yusof, SW Harun, Moh Yasin, Optik **173**, 180 (2018).
[15] M. A. M. Johari, M. I. M. A. Khudus, M. H. B. Jali, Al Noman, S. W. Harun, Optik **185**, 558 (2019).
[16] M. A. M. Johari, M. I. M. A. Khudus, M. H. B. Jali, M. S. Maslinda, U. U. M. Ali, S. W. Harun, A. H. Zaidan, R. Apsari, M. Yasin, Sensing and Bio-Sensing Research **25**, 100292 (2019).
[17] H. H. M. Yusof, S. W. Harun, K. Dimyati, T. Bora, K. Sterckx, W. S. Mohammed, J. Dutta, IEEE Sensors Journal **19**(7), 2442 (2018).
[18] G. Nemova, R. Kashyap, Journal of Lightwave Technology **25**(8), 2244 (2007).
[19] G. S. Murugan, J. S. Wilkinson, M. N. Zervas, Optics Letters **35**(11), 1893 (2010).
[20] A. Chiasera, Y. Dumeige, P. Feron, M. Ferrari, Y. Jestin, G. Nunzi Conti, S. Pelli, S. Soria, G. C. Righini, Laser & Photonics Reviews **4**(3), 457 (2010).
[21] A. Matsko, A. A. Savchenkov, D. Strekalov, V. S. Ilchenko, L. Maleki, I. P. N. Progress Report **42**(162), 1(2005).
[22] M. J. Md Ashadi, A. K. Muhammad Imran Mustafa, J. Mohd Hafiz, Al Noman, S. W. Harun, Journal of Physics: Conference Series, IOP Publishing Ltd. **1371**, 8 (2019).
[23] H. H. M. Yusof, M. H. Jali, M. A. M. Johari, K. Dimyati, S. W. Harun, M. Khasanah, M. Yasin, IEEE Photonics Journal **11**(1), 1 (2019).
[24] M. Pöllinger, D. O'Shea, F. Warken, A. Rauschenbeutel, Physical Review Letters **103**(5) 053901 (2009).
[25] A. V. Veluthandath, S. Bhattacharya, G. S. Murugan, P. B. Bisht, IEEE Photonics Technology Letters **31**(3), 226 (2018).
[26] G. S. Murugan, M. N. Petrovich, Y. Jung, J. S. Wilkinson, M. N. Zervas, Optics Express **19**(21), 20773 (2011).
[27] N. M. Isa, N. Irawati, H. A. Rahman, M. H. M. Yusoff, SW Harun, IEEE Sensors Journal **18**(7), 2801 (2018).
[28] M. N. M. Nasir, G. S. Murugan, M. N. Zervas, IEEE Photonics Conference (IPC). **1**, 759 (2016).
[29] M. Cai, O. Painter, K. J. Vahala, Physical Review Letters **85**(1), 74 (2000).
[30] A. V. Veluthandath, P. B. Bisht, Journal of Applied Physics **118**(23), 233102 (2015).
[31] P. Bianucci, Sensors **16**(11), 1841 (2016).

*Corresponding author: johariashadi@gmail.com